Motional Quantum Ground-State Cooing of a Single Sodium Atom

Yichao Yu, Nicholas R. Hutzler, Jessie T. Zhang, Lee R. Liu, and Kang-Kuen Ni*
Department of Chemistry and Chemical Biology,
Harvard University, Cambridge, Massachusetts, 02138, USA
Department of Physics, Harvard University, Cambridge, Massachusetts, 02138, USA and
Harvard-MIT Center for Ultracold Atoms, Cambridge, Massachusetts, 02138, USA
(Dated: May 28, 2017)

We report Raman sideband cooling of a single neutral sodium atom to its three-dimensional motional ground state in an optical tweezer. Despite having a very large Lamb-Dicke parameter, high initial temperature and large differential AC Stark shift in the excited state, after applying a cooling sequence for a hundred milliseconds, we observed a ground state preparation fidelity of 70% using sideband thermometry. We demonstrated that Raman sideband cooling to motional ground state is applicable to systems where tight confinement or low initial cooling is hard to achieve. For example, the result provides new opportunities to achieve much lower temperatures in cold molecules with direct laser cooling.

Single neutral atoms trapped in optical tweezers provide a promising system for various applications including quantum information, quantum chemistry and quantum simulation of many-body systems. The interaction between different sites can be controlled by creating Rydberg excitation or by creating dipolar molecules from two trapped atoms. Combined with the ability to move, detect and manipulate individual sites, arrays of optical tweezers can be used to prepare complex interacting system with high fidelity. In order to achieve long coherence time and full quantum control of the system needed for these applications, it is usually necessary to control the thermal motion of the atoms by cooling to the three dimensional motional ground state in the optical tweezer, which has already been demonstrated with heavy alkali atoms including rubidium and cesium. However, some of the important properties of previous experiements, for example low initial temperature and small Lamb-Dicke parameter, may not be easily achievable for other systems and the versatility of this approach requires being able to perform ground motional state cooling in the more general case. In this letter, we present our work on cooling single sodium atoms trapped in optical tweezers to the motional ground state with Raman sideband cooling. Dispite having a large Lamb-Dicke parameter and high initial temperature, by utilizing several new cooling techniques and a well optimized cooling sequence, we are able to achieve a ground state probability of 80%.

The Raman sideband cooling we used to achieve the high ground state preparation fidelity consists of multiple cycles of laser pulses to manipulate the internal and motional states of the atoms. Figure 1A shows the schematic of the energy levels and the cooling sequence in our setup. Each cooling cycle starts with the sodium atom in the $|F = 2, m_F = -2\rangle$ ground electronic state and a certain vibration state n. In the first step, a Raman pulse drives a transition to the motional state $n - \Delta n$ to reduce the motional energy while also changing the internal state to $|F = 1, m_F = -1\rangle$. In the second step, which finishes the

cooling cycle, an optical pumping pulse bring the atom back to the $|F = 2, m_F = -2\rangle$ state to take away the entropy. The second step could also change the motional state of the atoms which could cause heating. The possibility for this to happen for an atom in the motional level n is approximately proportional to the effective Lamb-Dicke parameter $\eta_{eff}^{OP} = \sqrt{2n+1}\eta^{OP}$ where $\eta^{OP} =???$ is the Lamb-Dicke parameter for optical pumping. The geometry of the relevant beams (???and their polarizations) is showed in figure 1B. The optical tweezer has one weakly confined axial direction (axis 1) and two more strongly confined radial directions (axis 2 and 3). Multiple pairs of beams are used to drive the Raman transition during cooling in order to isolate and maximize the coupling to different trap axis.

Although Raman sideband cooling to motional ground state has already been successfully implemented on neutral atoms in other experiments using heavier species like Rubidium [????] and Cesium [????], such experiments generally use good polarization gradient cooling and a tight confinement to achieve a small Lamb-Dicke parameter and effective Lamb-Dicke parameter. However, this regime is harder to achieve with sodium atoms, creating additional challenges for us to realize ground state cooling. On the other hand, since these conditions can also be difficult to meet for other interesting systems like directly laser cooled molecules, the techniques we use to overcome these challenges could be useful for a wider variety of systems.

As mentioned previously, in order to perform Raman sideband cooling efficiently and minimize the heating during the optical pumping, we need to have a low initial temperature and a small Lamb-Dicke parameter. However, since the Lamb-Dicke parameter η is inversely proportional to $\sqrt{m}$ (???) where m is the mass of the atom, it is larger for sodium given the same trap depth (???). With $45mW$ of power at the focus of the trap, we measured a trapping frequency of $\{\omega_1, \omega_2, \omega_3\}/2\pi = \{67, 420, 580\}$ kHz which corre-
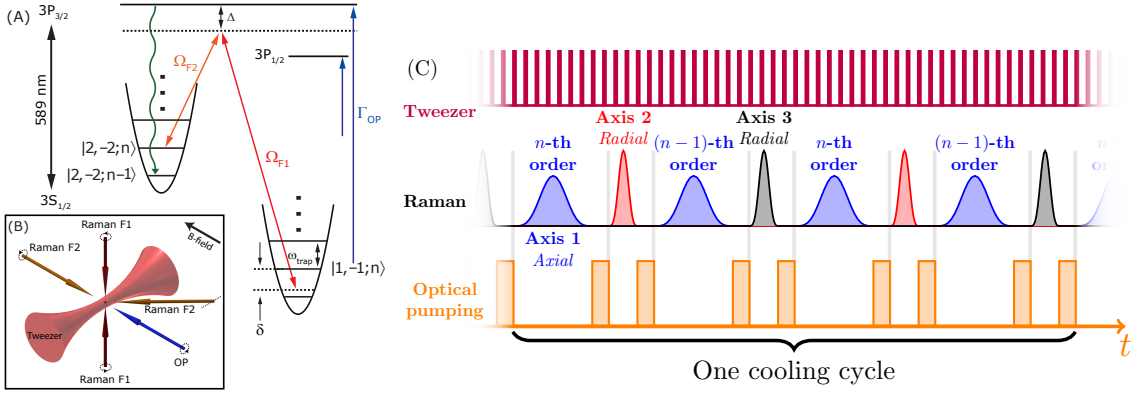
FIG. 1. (A) Energy levels and schematics of Raman sideband cooling. The Raman transitions has a one photon detuning $\Delta = 25GHz$ from the D2 line. We use D1 light with σ^- polarization to repump atom out of $|F = 2, m_F = -1\rangle$ state to minimize heating on the atom in $|F = 2, m_F = -2\rangle$ state. (B) Geometry and polarizations of the Raman and optical pumping beams relative to the optical tweezer and bias magnetic field. (C) Schematics of the cooling sequence. The tweezer is switching at $3MHz$ to reduce light shift during optical pumping. Each cooling cycle consists of 8 pulses. The four axial pulses are addressing two neighboring cooling orders. The two pulses in each radial directions are either addressing two neighboring cooling orders or having different length on the first order when most of the population are below $n = 3$ towards then end of the cooling sequence.

sponds to optical pumping Lamb-Dicke parameters of $\{\eta_1^{OP}, \eta_2^{OP}, \eta_3^{OP}\} = \{???, ???, ???\}$. Moreover, due to the unresolved(?) hyperfine structure in the $3^2P_{3/2}$ manifold, the sub-Doppler cooling in sodium is also less efficient and we start the Raman sideband cooling with a initial temperature of $40\mu K$. Combined with the high Lamb-Dicke parameters, this gives us a initial effective optical pumping Lamb-Dicke parameters of
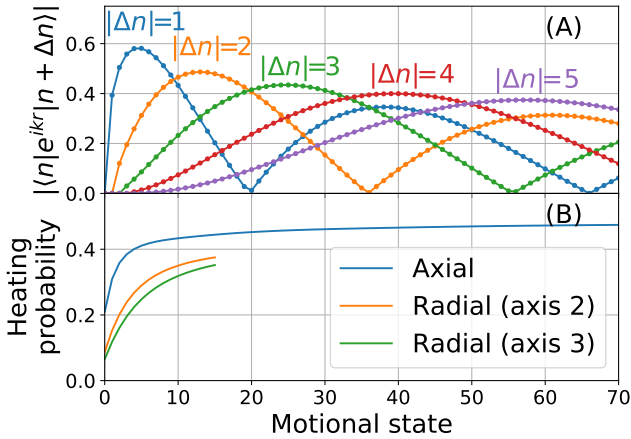

FIG. 2. Matrix elements and heating probabilities as a function of motional state. The range plotted covers 99% of the initial thermal distribution. (A) Matrix elements for Raman transition in the axial direction showing diviation from $\sqrt{n}$ scaling and multiple minimums for different sideband orders. (B) Heating probability during the optical pumping step for all three axis. Due to the large Lamb-Dicke parameter, there is a high probability of heating especially in the axial direction.

$\{\eta_{1eff}^{OP}, \eta_{2eff}^{OP}, \eta_{3eff}^{OP}\} = \{???, ???, ???\}$ As a result, there is a very high probability of heating during the optical pumping step (figure 2B) causing a 30% average heating probability during optical pumping in the weakly confined axial direction. Fortunately, the high Lamb-Dicke parameters also provide us tools to overcome this issue. From our geometry, the Lamb-Dicke parameters for Raman transitions are $\{\eta_1^R, \eta_2^R, \eta_3^R\} = \{???, ???, ???\}$. As shown in figure 2A, the high Raman Lamb-Dicke parameters causes a strong coupling to higher orders of cooling sidebands, especially for high motional states. This enables us to cool atoms in high motional states by driving on high order Raman sidebands, removing more motional energy in a single cooling pulse and offsetting the effect of strong heating. Since the heating probability is higher for high motional states, cooling on these high order sidebands can greatly suppress the high heating during optical pumping during the initial cooling. Since the coupling strength of different orders do not reach their minimums at the same time, using multiple orders of motional sidebands for cooling also avoids accumulation of population near the coupling minimum of a particular order, which improves the overall efficiency of the cooling process.

In additional to improving the cooling efficiency, the large Raman Lamb-Dicke parameters η^R also creates difficulties for measuring the temperature. Traditional sideband thermometry uses the ratio of the cooling and heating sidebands to measure $\bar{n}/(\bar{n}+1)$, which relies on the coupling strength to be proportional to $\sqrt{n}$. However, since we are not in the Lamb-Dicke regime, the coupling strength deviates from this simple scaling rule quickly as already shown in figure 2A, causing the normal sideband thermometry to break down. In order to solve this problem, when the atom temperature is still high, we
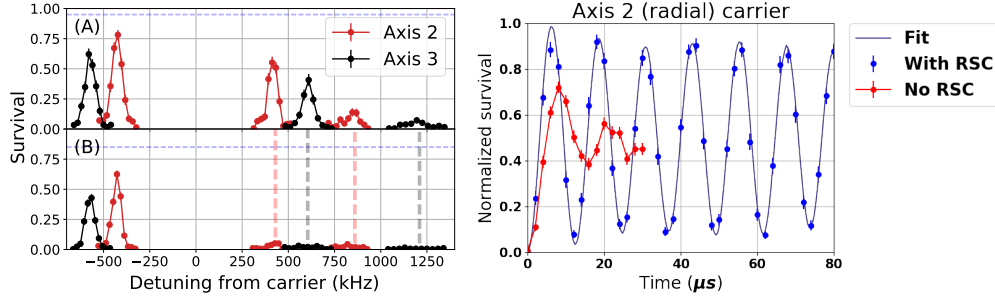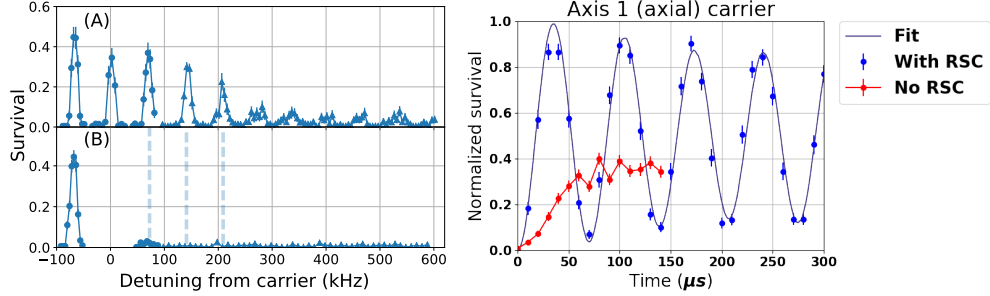
FIG. 3. (A) (B)

FIG. 4. (A) (B)

measure the heights of multiple sidebands to make sure no population is hidden at the minimum of one sideband order. And when the atom is cooled down, we estimate the temperature and ground state population under the assumption that only a few states are populated. This result is then verified using independent measure of Rabi flopping on the carrier and heating sidebands since they provide more information about the distribution of coupling strength.

Another issue caused by the high initial temperature is trap anharmonicity. Although the potential near the center of a focused Gaussian beam can be approximated by a harmonic trap, when a large number of levels are populated due to high initial temperature the anharmonicity of the trap can lead to broadening of the sideband and decrease of the sideband signal. In our setup, this effect limits the Rabi frequency of the Raman pulse on the radial sidebands to be no lower than tens of kilo-Hertz in order to drive atoms in different motional states equally.

Finally, the deep trap that is needed to trap and image single sodium atom also creates a very large AC Stark shift in the excited state. For the trap depth we are using, the light shift in the center of the trap is as large as $300MHz$. In additional to creating a large and position dependent detuning for the optical pumping light, it also mixes the excited state state hyperfine levels, affecting the branching ratio and increasing the number of photons needed during optical pumping. Similar to our loading and imaging process [???], we solve this issue by switching the trapping light at $3MHz$ during the whole

cooling sequence. Due to the large light shift, the optical pumping is effectively off when the trap light is on. Since the atom can only be addressed by the optical pumping light when the trap light is off, the effect of light shift on optical pumping fidelity is suppressed.

Taking all the features of our system into account, we use a Monte-Carlo simulation to verify the validity of our method. In the simulation, we can observe the high heating rate due to the high Lamb-Dicke parameters and confirm that by using high order Raman sideband transition in the cooling sequence we can suppress this effect and reduces the motional energy of the atom faster. The simulation is also used to guide the optimization of the cooling sequence by exploring the large parameter space and finding a robust cooling strategy. As shown in figure (?), we found that instead of cooling on only one sideband order at a time, it is generally more efficient to alternate the cooling pulse between two neighboring orders (axial) or pulse lengths. A cooling sequence like this minimizes the accumulation of atom in a state not addressed by a particular Raman pulse parameter.

For the more tightly confined radial directions, we starts the cooling with $\{\bar{n}_2, \bar{n}_3\}$ =????, ????. The radial sideband spectra of the initial distribution is shown in figure 3A where we can clearly see the first order heating, first order cooling and second order cooling sidebands. After applying about 1000 cooling pulses cooling in all three dimensions starting with cooling on the radial second order, the Raman spectrum with the same parameter is shown in figure 3B, where the first and second order

cooling sidebands on both axis are suppressed. Given the absence of the second order cooling sideband, we can estimate the ground state probability in each direction based on the height of the first order cooling and heating sideband to be ???? and ????. Due to the complexity of the sideband structure, we measured the Rabi flopping on the carrier and heating sideband before and after cooling (3C and 3D) as a independent way to obtain the population in different motional states. Fitting the Rabi flopping data give a ground state probability of ???? and ????, showing good agreement between the two methods.

The axial direction is much less confined and therefore has a much higher initial effective Lamb-Dicke parameter of $\eta_{eff1}^{OP} \approx 3.3$. The line in figure 4A shows the Raman spectrum in the axial direction before applying Raman sideband cooling where we can see clearly resolved Raman cooling sidebands up to the eighth order suggesting that we have many motional states populated in this direction. Therefore, we starts our cooling sequence by driving Raman transitions on the eighth order axial cooling sideband. After applying the cooling sequence identical to the one we use to cool the radial directions, the spectrum is shown as the blue line in figure 4A. All of the high order ($\geqslant 2$) axial cooling sidebands disappeared and the first order cooling sideband is also strongly suppressed. The ground state probability calculated from this spectrum is ????. We can also use Rabi flopping on the carrier and heating sideband to varify this result similar to the radial direction. In this case, we see very good agreement on the carrier (figure 4B) but there is additional decoherence on the axial first order heating sideband (figure 4C). We believe this decoherence is caused by technical noise in our setup which produces the strongest effect on this transition due to its slow Rabi frequency. The decoherence time scale agree with the magnetic field fluctuation we measured which produces a Zeeman shift of around $5kHz$.

Combining the axial and radial cooling results, we have achieved a ground state probability of ..... We believe this is currently limited by off-resonant scattering from the Raman beams and the resonance shift caused by magnetic field fluctuation. Improvements on these should improve the cooling performance even further.